

---

# Assessing the Challenges of Urban Flood Modelling: A TELEMAC-2D Rain-on-Grid Framework to Quantify the Relative Impacts of Surface Calibration, Infrastructure Modelling and Operational Rules in the Emscher Catchment

---

[Jens Reinert](#)\*, [Julian Hofmann](#), [Adrian Almoradie](#), [Catrina Brüll](#)

Posted Date: 26 February 2026

doi: 10.20944/preprints202602.1552.v1

Keywords: urban flood modeling; TELEMAC-2D; rain-on-grid; hydraulic infrastructures



Preprints.org is a free multidisciplinary platform providing preprint service that is dedicated to making early versions of research outputs permanently available and citable. Preprints posted at Preprints.org appear in Web of Science, Crossref, Google Scholar, Scilit, Europe PMC.

Copyright: This open access article is published under a [Creative Commons CC BY 4.0 license](#), which permit the free download, distribution, and reuse, provided that the author and preprint are cited in any reuse.

Disclaimer/Publisher's Note: The statements, opinions, and data contained in all publications are solely those of the individual author(s) and contributor(s) and not of MDPI and/or the editor(s). MDPI and/or the editor(s) disclaim responsibility for any injury to people or property resulting from any ideas, methods, instructions, or products referred to in the content.

Article

# Assessing the Challenges of Urban Flood Modelling: A TELEMAC-2D Rain-on-Grid Framework to Quantify the Relative Impacts of Surface Calibration, Infrastructure Modelling and Operational Rules in the Emscher Catchment

Jens Reinert <sup>1,\*</sup>, Julian Hofmann <sup>1</sup>, Adrian Almoradie <sup>2</sup> and Catrina Brüll <sup>1</sup>

<sup>1</sup> Institute of Hydraulic Engineering and Water Resources Management, RWTH Aachen University

<sup>2</sup> Emschergenossenschaft und Lippeverband, 45128 Essen, Germany

\* Correspondence: reinert@iww.rwth-aachen.de; Tel.: +49 241 80 25747

## Abstract

Urban flood modelling in infrastructure-dense and heavily modified catchments requires enhanced process realism, operational applicability, robust diagnostic and scenario-based evaluation to reliably capture complex system interactions and support decision-making under extreme and failure conditions. This study employs a TELEMAC-2D rain-on-grid approach to simulate pluvial flood dynamics in two urban sub-catchments of the Emscher River (North Rhine-Westphalia, Germany). A stepwise model development and calibration workflow is implemented, combining and adjustments of land-use-based roughness, refinement of SCS Curve Numbers, and the progressive integration of key hydraulic and operational components, including culverts, bridges, retention basins, and pumping stations. Model performance is evaluated based on hydrograph shape and volume, peak discharge and its timing, and inundation extent, with a specific focus on the relative contributions of (i) surface parameter calibration (friction coefficient-Manning's  $n$  and run-off- Curve Numbers), (ii) explicit representation of hydraulic structures, and (iii) operational control rules under varying rainfall scenarios and antecedent moisture conditions (AMC). The analysis tests the hypothesis that structural and operational realism can contribute as much as traditional surface calibration to improve model performance and that their effectiveness is strongly influenced by prior wetness. Results shows that including retention basins and pumping stations along with operational rules significantly improves agreement with observed discharge. It shows systematic sensitivity and improvements across AMC scenarios with NSE values from -0.129 to +0.77, RMSE from 3.380 to 1.52  $\text{m}^3 \text{s}^{-1}$ , peak discharge errors from -6.20 to -0.49  $\text{m}^3 \text{s}^{-1}$ , and volume bias from -0.67 to +0.04. This shows that even with careful calibration of surface parameters (e.g., roughness and runoff coefficients), models that exclude infrastructure (e.g., pumps and retention basins) fail to accurately reproduce peak flows and recession behaviour. A targeted routing-focused calibration (R4) further reduced the remaining peak timing mismatch under saturated conditions, but introduced increased volume bias, indicating that residual discrepancies are primarily linked to simplified representation of fast urban conveyance pathways rather than surface parameterisation alone. Flood response is not determined by rainfall alone. Initial wetness and how infrastructure is operated can strongly and unpredictably change flood behaviour. Overall, the findings emphasise that for a complex and engineered urban environment, reliable urban flood simulations requires the combined consideration of hydrodynamic processes, hydrological initial conditions, and operational behaviour. The study provides practical guidance on the limits of calibration-only approaches and identifies when explicit representation of infrastructure and operational processes is essential for robust modelling.

**Keywords:** urban flood modeling; TELEMAC-2D; rain-on-grid; hydraulic infrastructures

## 1. Introduction

Extreme rainfall events of short duration and high intensity have increasingly highlighted the vulnerability of urban areas to flooding. Climate change is expected to further intensify these events, increasing risks for densely populated catchments where land surface variability, impervious surfaces, and critical infrastructure influence flood dynamics in complex ways [1–3]. In such environments, flood risk assessment and operational planning require models that can represent not only rainfall–runoff generation but also the effects of engineered structures like culverts, bridges, pumping stations, and retention basins on spatial flood patterns [4,5].

Hydrodynamic models have become crucial tools for simulating urban flood processes. Among them, TELEMAC-2D is popular in research and practice because of its flexible unstructured mesh and capability to incorporate rainfall directly at the grid level [6,7]. Rain-on-grid methods are particularly useful for event-based studies of flash floods since they avoid separate hydrological components and allow for distributed infiltration and roughness parameterization using Curve Numbers (CN) and Manning's  $n$  values [8,9]. While calibrating these parameters can improve the overall model fit, earlier studies have shown that neglecting infrastructure causes systematic biases in hydrograph simulation, especially in timing and peak discharge [10–12].

At the same time, hydraulic structures are often modeled very simply or left out entirely. Culvert, for instance, has been shown to significantly impact flow routing and backwater buildup, yet it is rarely included in urban flood models [13]. Pumping stations and retention basins are usually represented by static sink–source terms, even though their effectiveness depends heavily on operational rules [14–16]. This gap between structural realism and simplified parameter calibration has reduced the reliability of many urban flood models.

Another important factor is the role of antecedent moisture conditions (AMC), which control infiltration capacity and initial storage before an event. Studies have shown that AMC significantly impacts runoff generation and peak flows, even in developed catchments [17]. However, systematic analyses that integrate AMC variability with explicit infrastructure modeling are still rare.

This study aims to identify the relative impacts of (i) surface parameter calibration, (ii) explicit structural representations of culverts, bridges, pumping stations, and retention basins, and (iii) operational control rules under different AMC scenarios on the accuracy of TELEMAC-2D flood simulations. The case study focuses on the Emscher catchment in North Rhine-Westphalia, Germany: A heavily urbanized basin with extensive flood control infrastructure.

This work was carried out as part of the Interreg North-West Europe FlashFloodBreaker Project.s

## 2. State of the Art

Urban flood modeling has significantly improved over the past decades, driven by the need to better capture increasingly frequent and intense (flash) flood events. Major advances have focused on representing urban surface variability, enhancing rainfall–runoff coupling methods, and incorporating critical infrastructures into hydraulic models.

### *Urban Surface Representation and Calibration in 2D Flood Models*

Previous studies highlighted that imperviousness, building density, and micro-topography greatly influence urban runoff generation [2,3]. Calibration has usually depended on land-use dependent Curve Numbers (CN) and Manning's roughness coefficients (Mannings  $n$ ), adjusted to match observed hydrographs [8,9]. While these methods enhance model performance, they primarily focus on surface features and cannot account for the effects of engineered structures.

### *Rain-on-Grid Approaches for Urban Flood Modelling*

Hydrodynamic models like TELEMAC-2D are increasingly used for rain-on-grid simulation, enabling direct conversion of radar-based precipitation data into distributed runoff [6,7]. This method has shown to be effective in urban settings, especially for event-based flash flood analysis. Ensuring

numerical stability and proper mesh design remains essential, with recent research emphasizing how results can be sensitive to spatial resolution, solver configurations, and wetting–drying thresholds [18–20].

#### *Hydraulic Structures and Operational Infrastructure in Urban Models*

A growing body of research highlights the importance of hydraulic structures in influencing flood response. Culverts and bridges can restrict or redirect water flows, with clogging effects seen as especially important for floodplain connectivity [13]. Pumping stations and retention basins significantly influence hydrographs, although their operation is often represented only by simplified sink–source terms [16,21]. These simplifications can cause considerable errors in peak flow magnitude and timing [4,5,14].

Comparisons between calibration-focused and infrastructure-integrated models reveal that ignoring structural components often results in underestimating backwater effects and misrepresenting discharge peaks [10–12]. These results indicate that calibration alone cannot guarantee robust performance in urban catchments.

#### *Antecedent Moisture Conditions and Hydrological Initialisation*

Although runoff generation is well known to depend on initial wetness, explicit integration of AMC is mainly applied in hydrological modelling, while its use in urban flood models this remains limited. Hettiarachchi et al. [17] demonstrated that AMC significantly alters flood response even in developed basins, but systematic analyses combining AMC variability with infrastructure representation are scarce. This highlights an important gap in current research.

#### *Remaining Research Gaps and Positioning of This Study*

In summary, existing research has enhanced urban flood modeling through improved parameter calibration, advanced rain-on-grid techniques, and isolated analyses of hydraulic structures. However, no study to our knowledge far has systematically quantified the relative contributions of surface calibration, structural modeling and operational control under different antecedent moisture conditions within a TELEMAC-2D framework. Addressing this gap is the primary goal of this study. The novelty lies in combining stepwise calibration (CN, Mannings  $n$ ), explicit structural integration (culverts and bridges), and operational realism (pumping, retention basin control rules) under varying AMC conditions in a large-scale TELEMAC-2D setup.

### **3. Materials and Methods**

#### *3.1. Study Area and Hydrological Setup*

The study area is situated in the Emscher catchment in North Rhine-Westphalia, Germany, a highly engineered lowland river basin characterized by dense urbanization and extensive hydraulic infrastructure. The catchment has experienced significant hydromorphological changes over the past century, including channelization, separation of wastewater and stormwater flows, and the construction of numerous pumping stations and flood retention basins. These alterations have greatly changed the natural hydrological response, decreasing infiltration capacity and increasing the amount of surface runoff during heavy rainfall events.

Two representative urban sub catchments were selected: Rossbach and Ruepingsbach (**Figures 1 and 2**). They were chosen to represent contrasting hydrological and infrastructural conditions within the Emscher basin.

##### Rossbach:

- Catchment area size: 30.88 km<sup>2</sup>
- Average river slope: 2.6‰
- Average discharge amount: 0.360 m<sup>3</sup>/s



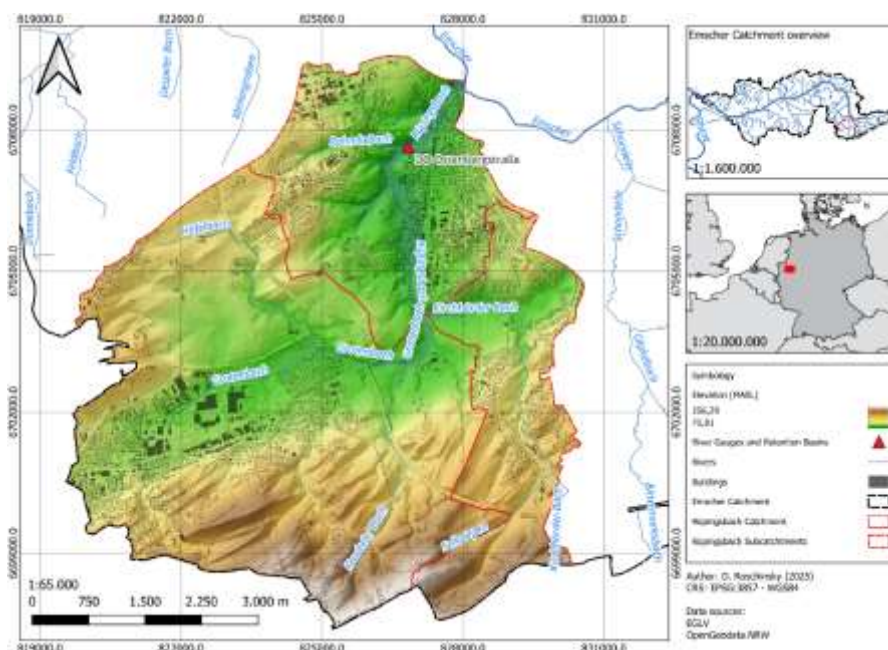


Figure 2. Subcatchment area of Ruepingsbach.

### 3.2. Digital Model Setup

The hydrodynamic simulations were conducted in TELEMAC-2D (version 8.4) using an unstructured triangular mesh and from a high-resolution (1m) digital elevation model (DEM). Pre-processing steps, including catchment delineation, mesh creation, and spatial parameter assignment (such as building representation), were performed in QGIS (version 3.40.5) and BlueKenue (version 3.3.4). The goal was to produce a physically accurate representation of terrain, land cover, and hydraulic structures suitable for simulating pluvial and fluvial flood dynamics in mostly urban areas.

#### 3.2.1. DEM, Mesh Design and Numerical Configuration

A 1-m resolution DEM (Geoportal NRW, 2018<sup>1</sup>) served as the topographic basis. Before mesh generation, the DEM was corrected for artefacts such as bridges, vegetation, and overpasses. River channels and depressions were reviewed to ensure hydraulic connectivity, while building footprints were introduced using the building-block method (Section 3.4.1).

The computational mesh was generated using a constrained Delaunay triangulation. Mesh density was varied according to hydraulic relevance:

- Main channels and culvert zones: ~1 m target edge length.
- Densely urbanized areas: ~3 m target edge length.
- Open fields and low-sensitivity areas: ~25 m target edge length.

Transitions between refinement zones are automatically smoothed by BlueKenue to avoid abrupt element size changes.

TELEMAC uses Finite Element Method (FEM) to solve the shallow water equations. For the model-set up, numerical stability was ensured through a variable time-stepping approach with a maximum Courant number of 0.9, fulfilling the Courant–Friedrichs–Lewy (CFL) condition. Advection of depth and velocity was computed using the method of characteristics (MOC) scheme, which, although typically recommended for tidal flat systems, was applied here to the inland Emscher catchment to enhance numerical stability and accurately capture advective transport, while no Streamline Upwind Petrov–Galerkin (SUPG) stabilization advection scheme was applied. The hydrodynamic equations were solved using a conjugate gradient solver, with a convergence

<sup>1</sup> [https://www.opengeodata.nrw.de/produkte/geobasis/hm/dgm1\\_tiff/](https://www.opengeodata.nrw.de/produkte/geobasis/hm/dgm1_tiff/)

tolerance of  $1.0 \times 10^{-4}$  and a maximum of 2000 iterations, consistent with the TELEMAC-2D defaults. Wetting and drying were handled with tidal flats enabled and a threshold depth of 0.05 m, which balances stability and physical realism during inundation and recession. Additional stability was achieved through negative depth correction, a free-surface gradient compatibility factor of 0.9 and full mass-lumping of the depth equation.

The modular coupling approach (Section 3.1) required explicit handling of lateral and downstream boundaries. Hydrographs extracted from upstream subcatchments were inserted as discharge inflows at predefined sections of the mesh. At the downstream end of each subcatchment, a free outflow boundary was applied. Initial water levels were set to zero depth across the floodplain.

### 3.2.2. Land Use and Soil Data

Land use data were obtained from the Geoportal NRW and supplemented by the ATKIS topographic dataset (Official Topographic-Cartographic Information System). These datasets provide spatially explicit information on land cover categories, which are essential for assigning hydrological and hydraulic parameters in the TELEMAC-2D model. Each land use class was linked to a Curve Number (CN) regarding its soil group and a Manning's roughness coefficient ( $n$ ) following standard hydrological classifications (Ligier, 2016; Broich et al., 2019).

To systematically test model sensitivity, three calibration levels (R1–R4) were defined. This process was carried out manually and not through an automated optimisation procedure:

- R1: Baseline values from literature and standard tables,
- R2: Intermediate adjustment based on catchment-specific observations,
- R3: Refined calibration against observed hydrographs.
- R4: Additional calibration against observed hydrographs after incorporating hydraulic components

**Table 1.** CN and  $n$  values for the calibration series R1 – R4.

Land use type	SCS-CN [-]				Mannings $n$ [ $s/m^3$ ] <sup>1</sup>			
	R1	R2	R3	R4	R1	R2	R3	R4
Forest	55	55	55	55	0.100	0.120	0.120	0.12
Sports, leisure and recreation area	68	70	72	72	0.040	0.060	0.080	0.08
Mixed use	75	78	82	83	0.060	0.080	0.100	0.095
Agriculture	78	78	80	80	0.050	0.060	0.080	0.08
Residential area	80	82	87	88	0.070	0.100	0.130	0.12
Grove	80	80	82	82	0.100	0.120	0.120	0.12
Unvegetated area	80	85	88	88	0.040	0.060	0.080	0.08
Cemetery	98	98	98	98	0.040	0.060	0.060	0.06
Industrial and commercial area	98	98	100	100	0.035	0.050	0.060	0.048
Special functional area	98	98	100	100	0.040	0.050	0.050	0.05
Road traffic	98	98	98	98	0.025	0.035	0.050	0.038
Square	98	98	100	100	0.040	0.050	0.060	0.045
Rail traffic	98	98	98	98	0.025	0.035	0.040	0.03
Lakes	100	100	100	100	0.040	0.040	0.040	0.04
Rivers	100	100	100	100	0.020	0.030	0.030	0.023

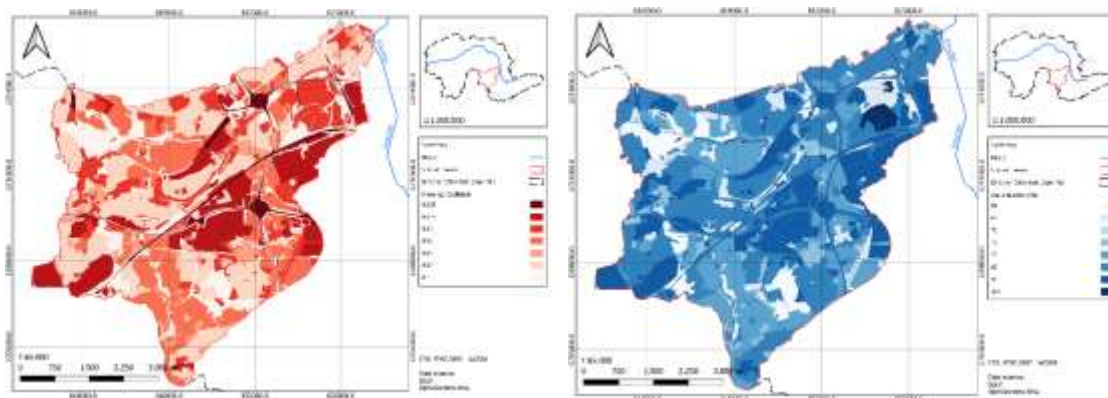


**Figure 3.** Roughness (left) and SCS-CN Curve Number (right) distribution of values in the Rossbach subcatchment area.

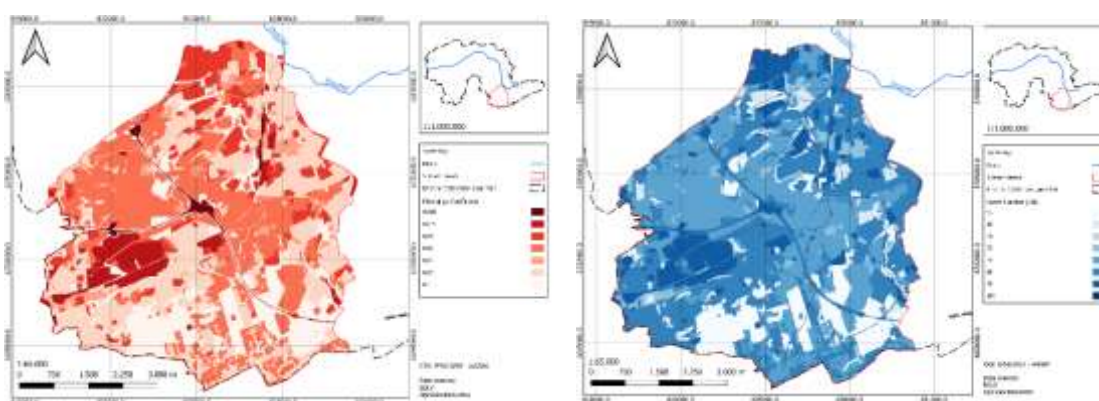


**Figure 4.** Roughness (left) and SCS-CN Curve Number (right) distribution of values in the Ruepingsbach subcatchment area.

### 3.2.3. Rainfall and Runoff Modeling

Rainfall data was obtained from the RADOLAN-RW product of the German Weather Service (DWD), which offers gauge-adjusted radar rainfall estimates at 1 km<sup>2</sup> spatial and 5-minute temporal resolution. The dataset was pre-processed in QGIS using the radolan2map plugin.

For model validation, a severe storm in June 2023 was selected. The event featured highly localized convective rainfall cells with peak intensities over 35 mm/h in several subcatchments and a total rainfall of 69.3 mm over 13 hours. This event was chosen because it caused observable flooding in multiple urban areas of the Emscher basin and had reliable gauge data available for validation. Gauge data were provided by EGLV.

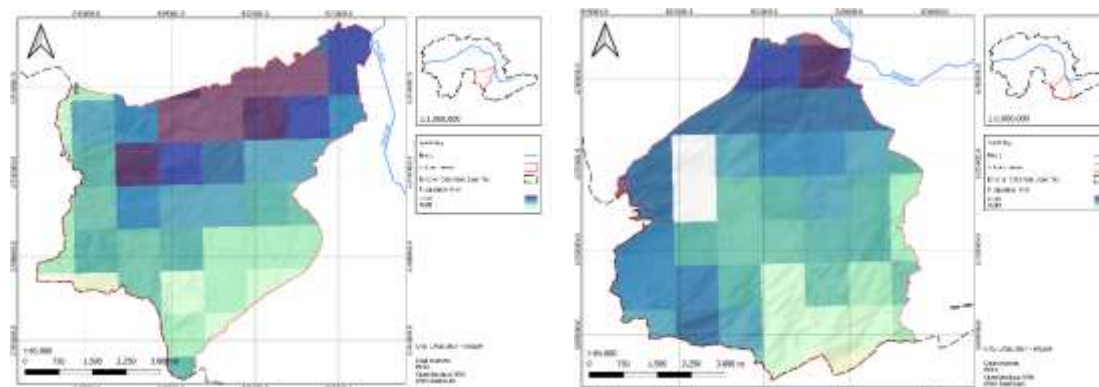


**Figure 5.** Precipitation sum of the 2023 rainfall event coming from the RADOLAN dataset by Germany Weather Service (DWD).

The rainfall–runoff transformation was directly integrated into TELEMAC-2D using a Rain-on-Grid method based on the Soil Conservation Service Curve Number (SCS-CN) approach. This method relates total precipitation to effective runoff through three main parameters: maximum potential retention (S), initial abstraction (Ia), and land-use-dependent CN values which were spatially assigned to each mesh element.

Three scenarios of antecedent moisture conditions (AMC) were explicitly incorporated by adjusting CN values according to SCS guidelines. Dry conditions (AMC I) correspond to lower CN values, indicating higher infiltration and storage capacity, while wet conditions (AMC III) lead to increased runoff due to limited retention capacity. In the TELEMAC-2D rain-on-grid workflow, this AMC I–III split is routinely implemented by selecting AMC-specific CN sets as defined by the SCS conversion rules.

A custom Fortran subroutine was created to load rainfall fields from temporally resolved ASCII files, which contain  $x$ ,  $y$ ,  $t$  coordinates and precipitation depths. The routine updates rainfall intensity at each mesh node for every model time step, allowing full spatiotemporal variability of the rainfall event. This implementation enables TELEMAC-2D to simulate short-duration, high-intensity storm dynamics that are critical for flash flood formation in urban catchments.

### 3.3. Urban Infrastructure Integration

Urban flood dynamics are heavily shaped by human-made hydraulic structures that control, redirect, or temporarily store water flow. To accurately represent these effects, key urban features, including buildings, sewer-related abstractions, culverts, bridges, retention basins, and pumping stations, were systematically incorporated into the TELEMAC-2D model. The objective was to ensure essential hydraulic realism while keeping computational demands manageable.

#### 3.4.1. Buildings

Building footprints were sourced from the Open Data Portal NRW and implemented using the building-block method. Impermeable polygons were vertically extruded and assigned artificially elevated terrain values in the mesh. This method prevents water from entering buildings and directs runoff along realistic urban routes such as streets and open spaces. It also helps maintain realistic runoff volumes near buildings. During high-intensity rainfall, local property drainage is likely to be capacity-limited, while sewer effects are already represented via the urban initial-loss formulation, so excess rainfall is plausibly redistributed around building footprints rather than removed from the domain. The extrusion height for modeled buildings was set to 3 m above the terrain. This representation is computationally efficient and reflects the primary role of buildings as lateral barriers, particularly important in low-gradient urban areas.

#### 3.4.2. Sewer System Abstractions

An explicit hydraulic sewer model was not available. Instead, sewer effects were approximated by spatially variable abstraction terms applied to impervious land-use classes (ATKIS dataset). A pre-processing routine was introduced to increase infiltration capacity in urban zones to mimic interception by stormwater inlets and underground pipes. Based on discussions with the waterboard in charge, the abstraction rate was set to  $10 \text{ mmh}^{-1}$  for the first 2 h. This simplification reduces overestimation of surface runoff in densely built areas, but does not reproduce dynamic sewer surcharges.

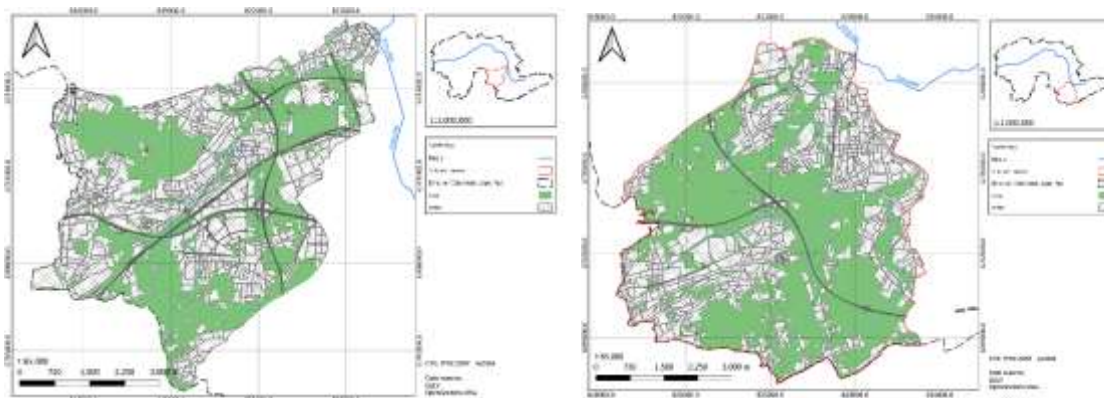


**Figure 6.** Distribution of the *urban fabric* (not green area) derived from the ATKIS Dataset as affected by the initial loss proxy method (sewer system).

### 3.4.3. Culverts and Bridges

Sixty six culverts and bridges were explicitly modeled using TELEMAC-2D's internal hydraulic structure modules. Each culvert was parameterized with inlet and outlet elevations, simplified cross-sectional geometry, length, and empirical head-loss coefficients based on [2]. The locations and dimensions data were provided by the waterboard EGLV. This structure-based approach allowed for the reproduction of local throttling effects, backwater buildup, and delayed flow transfer, which are crucial for accurately modeling urban flood wave propagation, especially under surcharge or debris-prone conditions. Although no explicit clogging scenarios were included in the current setup, the configuration permits the future addition of blockage routines.

Two modeling approaches were compared:

- Open configuration (OP): structures omitted, DEM cut through to allow unimpeded flow.
- Closed configuration (CL): explicit culvert/bridge modeling as hydraulic structures.

This allowed the evaluation of the hydraulic significance of culvert representation for flood routing and hydrograph reproduction.

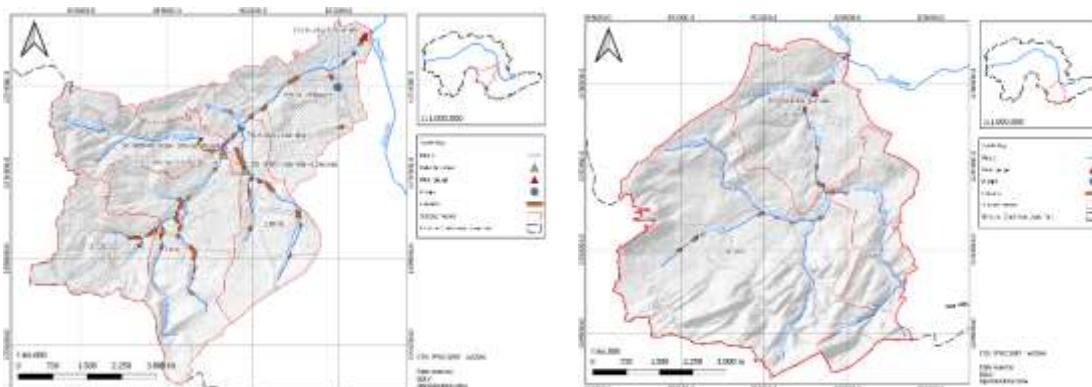


**Figure 7.** Locations of culverts and bridges in the subcatchment areas of Rossbach and Ruepingsbach.

### 3.3.4. Retention Basins and Pumping Stations

Retention basins were modeled as dynamic sink–source terms with specific storage capacities and outlet rules. Pumping stations were implemented through user-defined Fortran routines, where their activation depended on upstream water levels and official discharge; Head curves were provided by the local water authority EGLV.

- Retention basins: Two, with volumes of 151,000 m<sup>3</sup> and 58,000 m<sup>3</sup>
  - Operational rule: threshold-based activation

- Pumping stations: Two with rated capacities of [ $\sim 1 \text{ m}^3 \text{ h}^{-1}$ ].
  - Operational rule: event data-based control (Section 4.4).

This setup provided a realistic depiction of storage and controlled drainage, which are essential in lowland urban areas where gravity-driven outflow is limited.

To implement these process representations without modifying the TELEMAC-2D core, we relied on the standard user subroutine interface provided by the modelling system. As described in the TELEMAC-2D user manual, this mechanism offers predefined entry points for project-specific extensions, enabling transparent, version-compatible, and reproducible modifications of model behaviour. Accordingly, the operational logic was implemented using a set of adapted subroutines, summarised in **Table 2**.

**Table 2.** List of Subroutines Changed.

	Subroutine	Description
1	buse_c.f	Compute culvert discharge
2	lecbuse_c.f	Read culvert definitions and set orientation
3	culvert_algorithmus.F90	Interpolate flow and return discharge
4	culvert_module.F90	Define/read and store culvert data structures

The computer code for the subroutines developed in this study is openly available in a GitHub repository: <https://git.rwth-aachen.de/iww-public/telemac-urbandraincontrol>

### 3.5. Methodological Considerations and Impacts

Integrating urban infrastructure into TELEMAC-2D necessarily needs to balance hydraulic precision and computational efficiency. In this study, several simplifications were implemented to keep the model manageable while capturing the key flood processes.

Initially, the sewer network was not explicitly modeled but was represented through spatially variable abstraction losses in impervious zones. This approach minimizes early runoff overestimation but cannot simulate sewer surcharge or pipe capacity exceedance. The simplification is justified by the lack of reliable sewer data for the study area and the focus on aboveground flood dynamics.

Second, pumping stations and retention basins were utilized as source–sink systems with operational rules instead of detailed mechanical models. This approach allowed critical storage and pumping behaviors to be incorporated without making the setup overly complex. The downside is that energy use or redundancy could not be addressed in this model.

Third, culvert and bridge modeling relied on simplified geometric and empirical parameterizations. While sufficient to capture flow throttling and backwater effects, blockage by debris and sediment was not considered. This omission is important because clogging has been shown to significantly alter flood propagation during extreme events and should be tested in future scenario-based extensions.

Finally, the Rain-on-Grid approach using SCS Curve Numbers provided a practical compromise between hydrological detail and computational efficiency. While this method considers infiltration and antecedent moisture conditions, it does not explicitly model subsurface interflow or groundwater recharge, which may contribute to late hydrograph volumes.

Taken together, these methodological choices allowed the model to capture key flood dynamics at the urban scale, but they also introduce uncertainties. The trade-offs made in this study highlight the importance of transparently communicating assumptions, so results can be understood within the appropriate bounds of reliability.

## 4. Results

The calibration experiments evaluated how effectively surface parameter adjustments alone can replicate observed hydrographs. At the Rossbach gauge, simulated discharges could be directly

compared against available observed flow data, whereas at the Rüpingsbach gauge only water level observations were available for model evaluation. Three calibration levels (R1–R3) were tested, with R1 representing baseline values from literature, R2 including intermediate adjustments, and R3 providing refined tuning of Curve Numbers (CN) and Manning’s  $n$ . Each calibration level was applied in both the “open” (OP) and “closed” (CL) culvert configurations, resulting in six scenarios per catchment. To address the remaining temporal mismatch in peak discharge after surface-based calibration, an additional targeted calibration step (R4) was performed after integrating hydraulic components, focusing on flow routing efficiency rather than further adjustments to runoff generation parameters.

#### 4.1. Calibration Performance

At Rossbach, calibration enhanced the hydrograph shape but did not accurately capture peak discharges (**Figure 8**). Observed peak flows approached  $10 \text{ m}^3/\text{s}$ , while simulated peaks stayed between  $3.5$  and  $5.0 \text{ m}^3/\text{s}$  across all scenarios. Performance metrics (Table 4.1) confirm this underestimation: RMSE values ranged from  $2.9$  to  $3.4 \text{ m}^3/\text{s}$ , and peak errors ranged from  $-4.6$  to  $-6.0 \text{ m}^3/\text{s}$ . NSE values were close to zero, with slight improvements for OP scenarios (R1\_OP:  $0.137$ ; R2\_OP:  $0.157$ ; R3:  $0.011$ ), while most CL runs had negative NSE. The results indicate that calibrating surface parameters alone could not account for missing infrastructure effects, especially in dampening or delaying discharge peaks.

At Rüpingsbach, calibration significantly influenced both the magnitude and timing of simulated water levels (**Figure 8**). Baseline runs (R1) underestimated the flood peak by up to  $1.36 \text{ m}$  in OP mode, while R2\_CL greatly overestimated it ( $+1.02 \text{ m}$ ). R3\_CL provided the closest match to the observed peak, with an error of  $-0.43 \text{ m}$ , but overall NSE values remained negative across all scenarios (best: R3\_OP at  $-0.62$ ). RMSE values ranged from  $0.73$  to  $1.91 \text{ m}$ . These results suggest that surface calibration improved peak representation in some scenarios but did not consistently capture rising-limb dynamics, leading to systematic timing mismatches.

Calibration improved the local model's performance but did not consistently reproduce flood peaks or hydrograph shapes. Both catchments continued to show persistent under- or overestimation of peak magnitudes and negative NSE values despite parameter adjustments. The Rossbach results highlight peak underestimation, while the Rüpingsbach results display inconsistent performance, with both under- and overestimation depending on the configuration. These outcomes emphasize the limitations of calibration-only approaches in highly engineered urban catchments. The findings establish a baseline for subsequent analyses (Sections 4.2–4.4), where structural and operational components are explicitly integrated to improve model accuracy.

Catchment area	Scenario	NSE	RMSE	Peak Error
Rossbach	R1_CL	-0.138	$3.38 \text{ m}^3/\text{s}$	$-6.04 \text{ m}^3/\text{s}$
	R1_OP	0.137	$2.94 \text{ m}^3/\text{s}$	$-4.62 \text{ m}^3/\text{s}$
	R2_CL	-0.088	$3.31 \text{ m}^3/\text{s}$	$-5.76 \text{ m}^3/\text{s}$
	R2_OP	0.157	$2.91 \text{ m}^3/\text{s}$	$-4.58 \text{ m}^3/\text{s}$
	R3_CL	0.044	$3.10 \text{ m}^3/\text{s}$	$-5.07 \text{ m}^3/\text{s}$
	R3_OP	0.011	$3.15 \text{ m}^3/\text{s}$	$-5.47 \text{ m}^3/\text{s}$
Rüpingsbach	R1_CL	-1.772	$0.96 \text{ m}$	$-0.54 \text{ m}$
	R1_OP	-0.812	$0.77 \text{ m}$	$-1.36 \text{ m}$
	R2_CL	-10.000	$1.91 \text{ m}$	$+1.02 \text{ m}$
	R2_OP	-0.813	$0.77 \text{ m}$	$-1.42 \text{ m}$
	R3_CL	-1.945	$0.99 \text{ m}$	$-0.43 \text{ m}$
	R3_OP	-0.623	$0.73 \text{ m}$	$-1.33 \text{ m}$

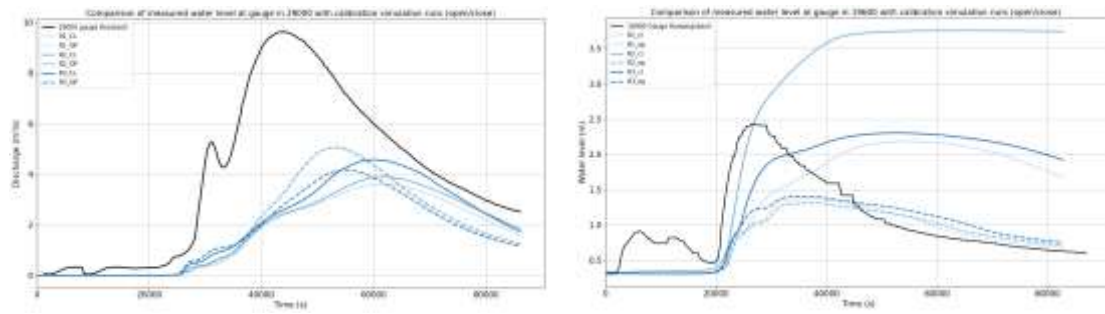


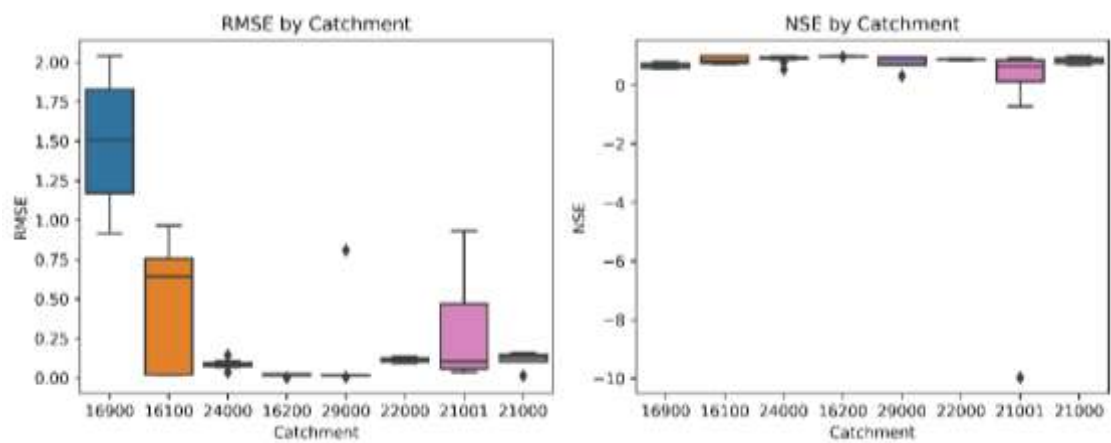
**Figure 8.** Observed and simulated discharges at Rossbach (Gauge 29000) and Rüeppingsbach (Gauge 19600) under calibration levels R1–R3, with open (OP) and closed (CL) culvert configurations.

#### 4.2. Influence of Hydraulic Structures

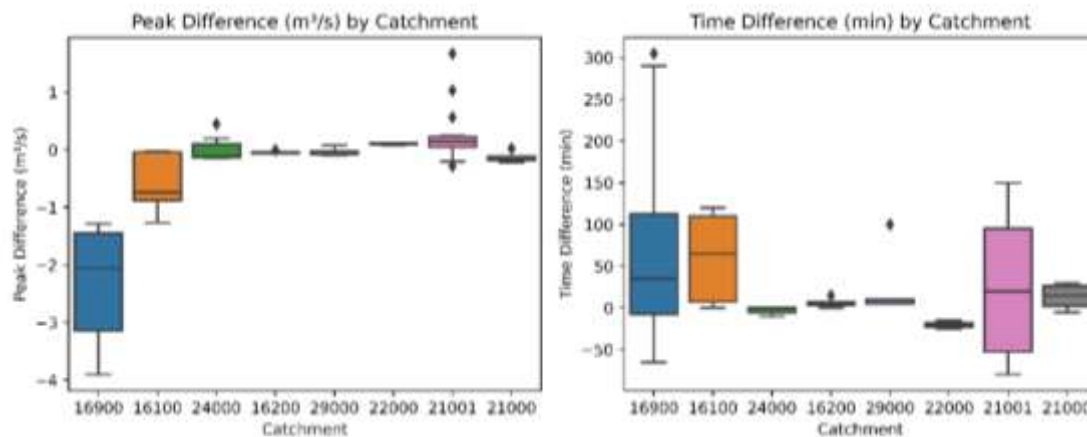
The effect of hydraulic structures was evaluated by directly comparing hydrographs from the open setup (DEM cut-throughs without structures) and the closed setup (explicit bridges and culverts using EGLV data, see Section 3.4.3). No observational dataset was used in this comparison; all performance metrics measure differences between the two modeling methods.

**Figures 9 and 10** show the results using Nash–Sutcliffe efficiency (NSE), root mean square error (RMSE), and differences in peak discharge magnitude and timing. These metrics were calculated pairwise for the same gauge locations, comparing simulated hydrographs from the open and closed configurations.

The boxplots show the distribution of metric values across all culvert and bridge locations. In most cases, the differences between setups were non-negligible, with RMSE values indicating changes in both peak magnitude and hydrograph shape. Peak timing differences ranged up to >300s, while peak discharge deviations reached ~3.9 m<sup>3</sup>/s. The interquartile ranges demonstrate that some structures exert only minor influence, while others cause pronounced differences between the two setups. Sub-catchments 21000, 22000, 24000, 21001 and 29000 belong to the Rossbach system, while all remaining sub-catchments 16000, 16200 and 16900 are part of the Rüpingsbach system.



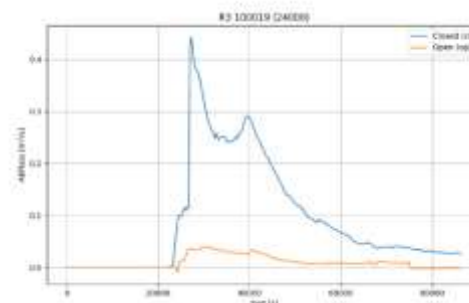
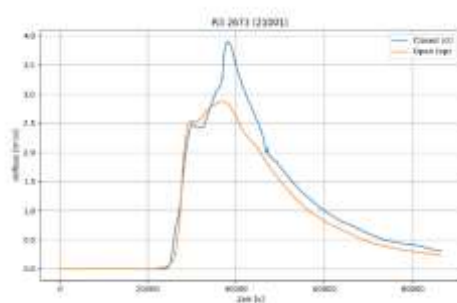
**Figure 9.** RMSE and NSE differences between open and closed configurations, grouped by subcatchment. (21000, 22000, 24000, 21001 and 29000 = Rossbach system; 16000, 16200 and 16900 = Rüpingsbach).



**Figure 10.** Absolute differences in peak discharge ( $\text{m}^3/\text{s}$ ) and peak timing (min) between open and closed hydrographs by subcatchment. (21000, 22000, 24000, 21001 and 29000 = Rossbach system; 16000, 16200 and 16900 = Rüpingsbach).

Selected hydrographs illustrate these findings in more detail (**Figure 11**):

- Culvert/bridge 2673 (Subcatchment 21001): Both setups reproduced similar rising limbs, but the closed configuration showed a sharper peak and slower decline, reflecting the influence of hydraulic constriction.
- Culvert/bridge 100019 (Subcatchment 24000): The difference was extreme, with the open run yielding almost no discharge, while the closed configuration generated a distinct peak of  $\sim 0.45 \text{ m}^3/\text{s}$ . This highlights the inability of DEM cut-throughs to reproduce conveyance capacity at this site.
- Culvert/bridge 2624 (Subcatchment 29000): The closed run produced a lower and delayed peak compared to the open run, with a smoother recession limb. The open setup overestimated the peak discharge and underestimated the duration of elevated flows.
- Culvert/bridge 200002 (Subcatchment 16100): Here, both setups showed similar peak magnitude and timing, with only minor differences in the falling limb, indicating limited structural influence at this location.
- Culvert/bridge 200014 (Subcatchment 16900): The divergence was most pronounced: the open setup produced a sharp peak of nearly  $6 \text{ m}^3/\text{s}$ , while the closed configuration attenuated this to  $\sim 3.5 \text{ m}^3/\text{s}$  and extended the recession phase.



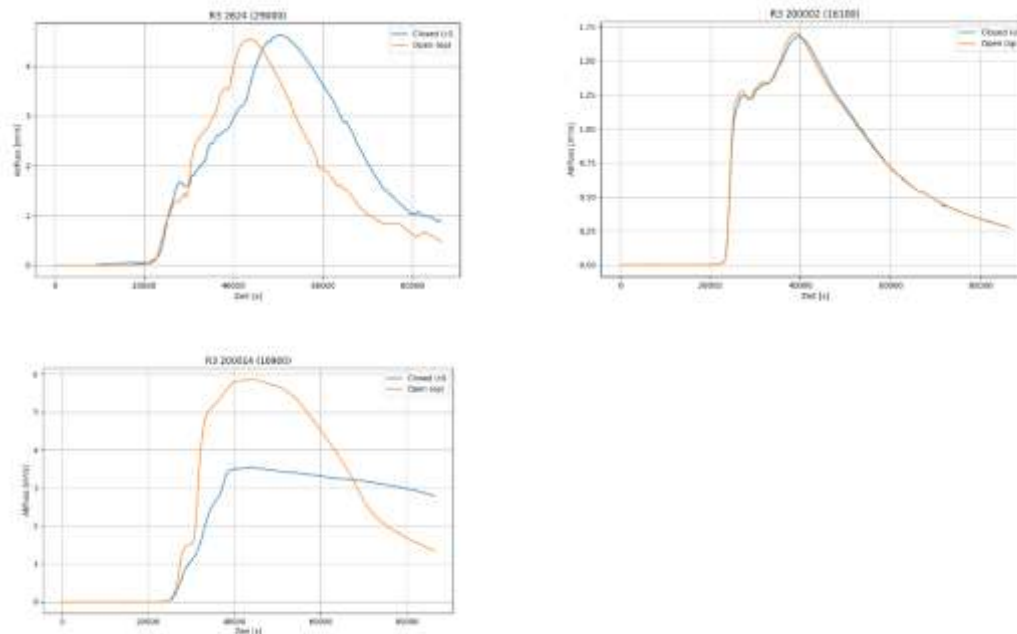


**Figure 11.** Simulated discharge hydrographs (R3 calibration) comparing open (orange) and closed (blue) setups at five locations: (a) Culvert/bridge 2624 (29000), (b) Culvert/bridge 2673 (21001), (c) Culvert/bridge 100019 (24000), (d) Culvert/bridge 200002 (16100), (e) Culvert/bridge 200014 (16900).

In summary, the boxplot analysis and individual hydrograph comparisons show that how culverts and bridges are represented has a clear and sometimes significant impact on model results. While in some areas the difference is small, in others, choosing between open DEM cut-throughs and explicit culvert modeling fundamentally alters hydrograph shape, peak levels, and timing.

#### 4.3. Effect of Retention Basins, Pumping Stations, and Antecedent Moisture Conditions

The results of Section 4.1 show that calibration and structural representation alone are not enough to accurately reproduce the flood dynamics observed in the Rossbach catchment. Even the refined R3 variants continue to display trade-offs between peak magnitude, timing, and event volume. To overcome these issues, retention basins and pumping stations were added to the model (R3+QP1), and the system's performance was assessed under different antecedent moisture conditions (AMC I–III).

**Figure 12** compares the observed discharge hydrograph with simulated responses under dry (AMC I), average (AMC II), and wet (AMC III) soil moisture conditions for the R3+QP1 configuration. The simulations reveal a clear sensitivity to antecedent wetness despite identical rainfall forcing and unchanged operational control rules. Under dry conditions (AMC I), the hydrograph peak is significantly underestimated, and the event volume is notably too low (peak error  $-6.198 \text{ m}^3 \text{ s}^{-1}$ ; volume bias  $-0.664$ ), while the peak occurs slightly earlier than observed (peak timing error  $0.583 \text{ h}$ ). Overall model performance remains modest, as indicated by an NSE of  $-0.129$  and an RMSE of  $3.380 \text{ m}^3 \text{ s}^{-1}$ .

Under average conditions (AMC II), overall agreement improves compared to AMC I (NSE  $0.551$ ; RMSE  $2.131 \text{ m}^3 \text{ s}^{-1}$ ), and the peak underestimation decreases (peak error  $-3.550 \text{ m}^3 \text{ s}^{-1}$ ). However, the simulated peak remains significantly delayed relative to the observation (peak timing error  $+3.167 \text{ h}$ ), and the event volume is still underestimated (volume bias  $-0.336$ ), indicating that antecedent wetness alone does not consistently resolve timing and storage–release dynamics.

The wet scenario (AMC III) demonstrates the best overall performance across metrics. It achieves the highest NSE ( $0.773$ ) and the lowest RMSE ( $1.515 \text{ m}^3 \text{ s}^{-1}$ ), with only a minor peak underestimation (peak error  $-0.492 \text{ m}^3 \text{ s}^{-1}$ ) and an almost balanced event volume (volume bias  $+0.038$ ). However, the peak timing remains delayed by several hours (peak timing error  $+3.417 \text{ h}$ ), indicating that while

higher antecedent wetness significantly enhances magnitude and volume representation, residual timing offsets still persist even with the infrastructure-augmented setup.

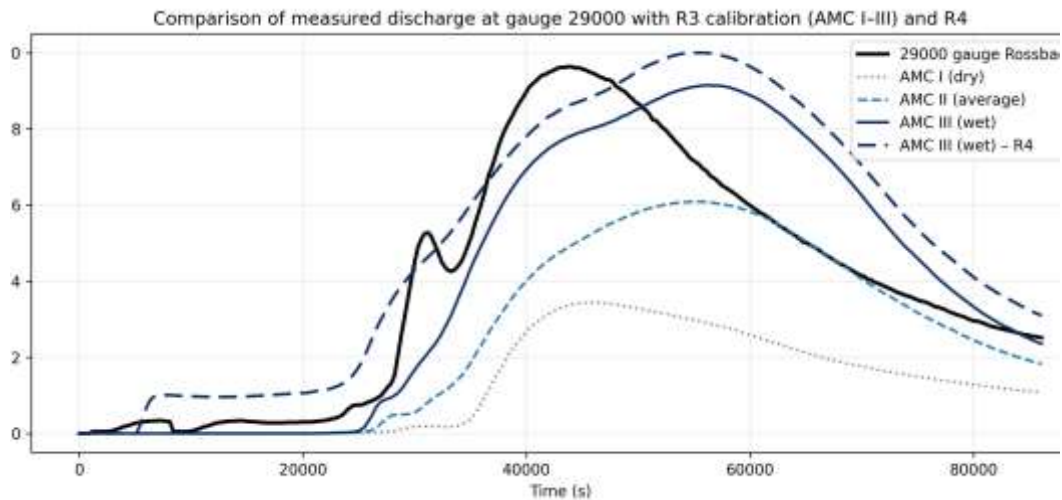


**Figure 12.** Simulation run R3 with integrated Retentions Basin and Pumps for dry (AMC I), average (AMC II) and wet (AMC III) soil moisture conditions. The additional R4 simulation represents an AMC III (wet) configuration with targeted routing calibration and is therefore labelled separately from the R3 AMC III run.

#### 4.4. Effect of Targeted Routing Calibration (R4)

To further address the remaining temporal mismatch in peak discharge identified in the AMC III scenario, an additional calibration run (R4) was performed using the refined R3 parameter set. In contrast to previous calibration steps, R4 focused exclusively on flow routing efficiency by selectively adjusting Manning's roughness coefficients in dominant transport corridors, while retaining the antecedent moisture condition (AMC III) and the overall surface parameterisation.

**Figure 12** includes the observed discharge hydrograph at gauge 29000 with the simulated responses for the R3 calibration under AMC I–III conditions and the additional R4 run. In the R3 AMC III configuration, the R4 simulation shows a clear shift in the hydrograph towards earlier peak timing, while maintaining a comparable overall shape. The rising limb becomes steeper, and the peak occurs closer to the observed timing, indicating an acceleration of wave propagation through the urban drainage network.

Quantitative performance metrics for the R4 run are summarised in Table 3. Compared to the R3 AMC III scenario, the peak timing error is reduced, while the peak magnitude slightly exceeds the observed value (peak error  $+0.36 \text{ m}^3 \text{ s}^{-1}$ ). The overall model skill remains high, with an NSE of 0.69 and an RMSE of  $1.79 \text{ m}^3 \text{ s}^{-1}$ . The event volume is overestimated in the R4 configuration (volume bias of  $+0.29$ ), reflecting an increase in effective hydraulic connectivity due to the reduced routing resistance.

Overall, the R4 calibration results demonstrate that targeted adjustments of routing-related roughness parameters can substantially influence hydrograph timing and peak development without altering the underlying runoff generation processes. This additional calibration step, therefore, provides a complementary improvement to the AMC III configuration by further reducing temporal discrepancies between simulated and observed flood responses.

**Table 3.** Calculated evaluation metrics for Gauge 29000 (Rossbach) in the R3+QP1 scenario (+ AMC III R4) under various AMC conditions.

Scenario	R <sup>2</sup>	NSE	RMSE [ $\text{m}^3/\text{s}$ ]	Peak error [ $\text{m}^3/\text{s}$ ]	Peak timing error [h]	Volume bias [-]
AMC I	0.830	-0.129	3.380	-6.198	0.583	-0.664
AMC II	0.748	0.551	2.131	-3.550	3.167	-0.336

<b>AMC III</b>	0.812	0.773	1.515	-0.492	3.417	0.038
<b>AMC III (R4)</b>	0.790	0.686	1.785	+0.363	3.250	0.291

## 5. Discussion

### 5.1. Implications for Calibration and Validation

Improvements from R1 to R3 demonstrate the critical role of curve number and Manning's  $n$  parameterization in determining discharge volume and hydrograph shape. Despite adjustments, differences in hydrographs, particularly in total volume, recession rate, and timing, still exist.

The representation of hydraulic structures influences model accuracy. Incorporating structures explicitly, such as culverts and bridges, improves peak-flow and rising-limb predictions by simulating real-world delays. Open configurations, where structures are modeled as depressions, allow for faster flow, whereas closed setups, which create backwater effects, align more closely with actual conditions. These results highlight the hydraulic importance of structural details, especially in urban or complex terrains. [4,21].

The consistent underestimation of total volume indicates the omission of runoff components. In TEZG 29000, the absence of modeled pumping infrastructure likely led to volume deficits, since real pumps remove water and delay peaks. Excluding this component reduces the model's ability to simulate late-stage hydrograph features accurately.

Subsurface processes, such as interflow, also play a significant role, but are not represented in TELEMAC-2D's surface-based, CN-derived setup. This omission may explain the observed rapid recession curves, even in the optimal R3\_CL case.

Increasing  $n$ -values improved water retention, but some land-use types, notably urban areas with mixed surfaces or riparian zones with high roughness, remain underrepresented. A more detailed parameterization could better capture hydrodynamic feedbacks across different surfaces.

The additional R4 calibration further illustrates the limitations of surface-based parameter adjustment when peak timing discrepancies persist under saturated conditions. By selectively reducing Manning's roughness in dominant transport corridors while keeping antecedent moisture and runoff generation unchanged, the R4 run demonstrates that hydrograph timing is highly sensitive to effective routing resistance. Although peak timing improves compared to the R3 AMC III configuration, this comes at the cost of increased discharge volumes and partial peak overestimation. This highlights that manual roughness calibration can compensate for missing conveyance pathways only to a limited extent and risks conflating routing effects with runoff generation processes if applied beyond physically plausible bounds.

Ultimately, model accuracy depends on hydrological and hydraulic enhancements: explicit infrastructure modeling, inclusion of lateral flows, and refined land use roughness parameters. These improvements would enhance volume estimates, timing, peak predictions, and retention, especially during extreme rainfall events.

The automatization of calibration processes is increasingly recommended to address the complexity and high dimensionality of urban flood models. Automated approaches, for instance through optimization algorithms, multi-objective calibration frameworks, or machine-learning-based parameter tuning, enable a more systematic exploration of parameter space and reduce subjectivity in manual calibration. Such methods improve reproducibility, accelerate the calibration workflow, and enhance model robustness across a wide range of hydrological conditions. It is necessary to avoid overfitting during optimisation and maybe set a sensible threshold of parameters. In particular, automated calibration based on a data assimilation algorithm can help to capture nonlinear interactions between land-surface parameters, drainage components, and hydraulic infrastructure, which is essential for reliable flood forecasting and scenario-based stress testing (Hao, 2024).

Beyond parameter calibration through Curve Numbers and roughness coefficients, flood model validation in urban areas also benefits from spatial comparison with observed inundation extents.

Especially in settings lacking reliable gauge data, orthophotos, hazard maps, social media data or reports of affected infrastructure can provide valuable references. These spatial benchmarks help to detect mismatches between modeled and actual flood extents [12], particularly in morphologically challenging areas where microtopography, building density [11] or unaccounted drainage components strongly influence flow patterns [9].

In such cases, spatial validation complements hydrograph-based calibration by addressing not only the volume and timing of discharge but also the geographic accuracy of flood propagation. This is particularly important in anthropogenically altered environments where terrain and land use changes are often underrepresented in DEMs. Integrating both point-based and area-based validation strategies can thus enhance model robustness, especially for short-duration, high-intensity urban flood events.

### *5.2. Representation of Buildings and Urban Flow Constraints*

Using buildings as flow-relevant obstacles via the building-block method effectively captures how urban structures influence hydrodynamics in the TELEMAC-2D model. In dense residential and industrial areas, buildings significantly change local flow patterns, especially during pluvial flood scenarios. Assigning buildings as impermeable polygons above ground level allows the simulation to show key effects like lateral flow diversion, formation of preferred pathways (such as streets), and temporary pooling in urban depressions. These effects, crucial for localized flooding analysis, cannot be fully represented by terrain data alone, especially when high-resolution LiDAR simplifies building footprints or overgeneralizes vertical features.

The impact of buildings is most evident in areas with complex infrastructure and low gradients, where lateral flow restrictions and frictional variations govern runoff. Ignoring building effects here results in unrealistic flood extent and depth estimates and misplacement of flow accumulation zones. Thus, the building-block method enhances not just flow velocity representation but also the spatial distribution of flood impacts. Nevertheless, some limitations remain. Treating buildings as fully impermeable ignores partial permeability features like basements or open courtyards, and neglects building-specific resistance factors such as staggered facades or ventilation gaps. The lack of explicit drainage pathways, like curb-and-gutter systems or underground sewer pipes, reduces realism in subsurface, surface interactions, which are crucial in urban flood dynamics. Additionally, representing building-induced blockage without modeling vertical connectivity can overestimate restrictions at structures like bridges or passageways, causing artificial ponding and flow diversion.

Future improvements could include hybrid models that combine the building-block approach with semi-permeable wall representations, resistance layers, or coupled sewer flow modules. Incorporating open data and building metadata, such as ground floor elevation, footprint type, and usage, can further improve the hydraulic accuracy of urban flood simulations.

### *5.3. Implications of Culvert Representation in Urban Flood Modeling*

The results in Section 4.2 highlight the importance of explicitly including culverts and bridges in hydrodynamic flood modeling frameworks. Improvements in statistical performance measures, such as peak timing, hydrograph shape, RMSE, and NSE, demonstrate the hydraulic significance of these structures at both local and catchment levels. The findings align with previous studies such as Ah-Woane et al. [13], which emphasize the role of culverts and bridges as key flow control elements during high-intensity events.

The observed differences can be explained by two methodological factors. First, DEM cut-throughs involve arbitrary choices for incision width and depth, which often do not accurately reflect actual conveyance capacity. Second, although TELEMAC-2D's culvert routines allow for explicit parameterization, their effectiveness depends on input accuracy and the flow regime; simplified 1D assumptions may still cause deviations. These limitations highlight the importance of cautious interpretation of structure-related improvements.

Sensitivity varied across the study area. In infrastructure-dense, low-gradient subcatchments such as 21001 and 24000, explicit structures fundamentally changed hydrograph dynamics, shifting peaks, extending recession limbs, and reproducing multi-peak responses that were absent in the open setup. In contrast, steeper or hydraulically simpler regions (e.g., 22000 and 29000) exhibited only moderate sensitivity, as topographic gradients mainly controlled flow routing. Nevertheless, even in these areas, including structural features improved timing accuracy and decreased simulation spread, which is helpful for short-lead-time forecasts.

Overall, the results confirm that DEM-based cut-through approaches are inadequate for capturing the dynamic behavior of infrastructure-constrained flow paths. In urban and peri-urban catchments, ignoring culvert hydraulics can systematically underestimate upstream water levels and overstate downstream discharges, resulting in distorted hazard maps, biased design discharges, or poorly informed protection plans.

Future modeling should therefore incorporate culvert inventories more systematically, supported by detailed structural attributes and blockage susceptibility assessments. Implementing blockage scenarios, whether probabilistically or deterministically, would further improve robustness during extreme events. Additionally, interactions between culvert performance, upstream land use, and temporal rainfall patterns require deeper investigation, especially in small, fast-responding urban catchments.

#### 5.4. Implications for Retention Basins and Pumping Stations

The comparison of hydrograph responses across different modelling configurations shows that the effectiveness of flood mitigation infrastructure depends not only on its structural design but also, crucially, on the implementation of realistic operational logic. While refined surface parameterisation and structural integration enhance specific hydrograph characteristics, they do not fully capture the system behaviour of infrastructure-led urban catchments. This becomes particularly evident under saturated antecedent conditions (AMC III), where discharge magnitude and event volume can be reproduced with high skill, yet a persistent peak lag remains. This indicates that fast conveyance pathways typical of dense urban drainage are still underrepresented when the sewer system is simplified.

Although the R3\_CL calibration series improves peak timing and hydrograph shape through better land-use parameterisation and explicit representation of culverts and bridges, it consistently underestimates total discharge volumes. This systematic shortfall indicates that surface-based calibration alone is insufficient in urban settings where internal drainage mechanisms, such as controlled storage, pumping, and rapid conveyance through the minor drainage network, regulate not only late-stage runoff dynamics and recession behaviour but also the timing of the rising limb and peak.

The explicit inclusion of retention basins and pumping stations (**Figure 12**) fundamentally changes the simulated hydrograph response. Retention basins reduce peak discharges by temporarily storing runoff, while pumping stations redistribute discharge over time by delaying the return to baseflow. As a result, hydrograph volumes increase and recession limbs become smoother and more realistic. These effects are especially noticeable under different antecedent moisture conditions, emphasising the importance of system state in determining infrastructure efficiency. However, while retention and pumping strongly shape volumes and recession behaviour, they do not necessarily eliminate peak timing biases if upstream runoff conveyance remains dominated by surface routing due to simplified sewer representation. In low-lying urban areas where gravity-driven drainage is limited, such operational controls play a key role in flood management.

The targeted routing calibration applied in the R4 run further supports this interpretation. Despite the inclusion of retention basins and pumping stations, a residual peak delay under AMC III conditions persisted, prompting a selective reduction of surface roughness in high-connectivity zones. The resulting improvement in peak timing confirms that rapid conveyance through the minor drainage network remains underrepresented when sewer processes are simplified. At the same time,

the associated increase in event volume demonstrates that routing-focused roughness adjustments alone cannot substitute for explicit representation of sewer–surface exchange and fast transport pathways without introducing structural bias.

Importantly, the results indicate that pumping station performance is highly sensitive to the chosen operational scheme. Simplified activation rules based solely on local surface water presence (e.g., node-based thresholding) can misrepresent discharge dynamics, particularly under saturated conditions (AMC III). In contrast, implementing pumping behaviour using discharge–head relationships derived from real infrastructure specifications significantly enhances model performance. This method more accurately reflects real-world operational practices, where pumping may commence proactively or continue beyond local surface flow conditions to safeguard downstream infrastructure and uphold system functionality. In practical terms, operational realism improves how much water is released and how long drainage persists, whereas peak timing also depends on how fast runoff reaches control points, an aspect that is strongly influenced by surface–sewer connectivity and transport capacity.

From a flood risk management perspective, these findings are highly significant. Ensuring operational realism in model configurations is crucial when simulations support real-time decision-making, early warning systems, or emergency response planning. Poor representation of pumping logic can result in overestimated surface ponding, delayed forecasts, or an underestimation of peak mitigation capabilities, thereby diminishing the reliability of model-based risk assessments.

Furthermore, the strong interaction between antecedent moisture conditions and pumping effectiveness emphasises the need for scenario-based stress testing. Under saturated catchment conditions, even minor differences in pump activation thresholds or control curves can cause significant changes in peak attenuation, hydrograph timing, and flood extent. This underlines the importance of assessing operational infrastructure not just under isolated design conditions but across a variety of plausible system states.

In summary, this research shows that realistic urban flood modelling requires both structural and operational accuracy. Retention basins and pumping stations must be represented not just geometrically, but also functionally, using system-specific operational rules that mirror real-world management practices. Such dual-level integration is vital for producing robust, physically consistent simulation results that can inform risk-based flood management and scenario-driven resilience assessments in urban settings.

These findings also affect transferability. Parameter sets that perform well in one sub-catchment may not directly generalise to neighbouring basins if surface parameters implicitly compensate for local drainage connectivity. Improving the functional representation of the minor drainage system, through tighter coupling or reduced-order sewer–surface exchange, should increase parameter identifiability and thereby support more robust transfer of calibrated configurations to adjacent urbanised sub-catchments.

## 6. Conclusions

This study shows that urban flood modelling in highly engineered catchments needs a level of realism that goes beyond traditional surface-based calibration. While adjustments to Curve Numbers and Manning's roughness coefficients improve the overall shape of simulated hydrographs, they cannot, by themselves, fix key process limitations in infrastructure-rich urban catchments. In particular, remaining peak timing biases under saturated initialisation (AMC III) suggest that parameter refinement cannot replace missing or simplified internal drainage and conveyance processes. These findings demonstrate that parameter calibration alone cannot fully capture the interactions between hydrological states and engineered urban systems, where drainage connectivity, operational controls, and routing constraints jointly influence hydrograph magnitude, recession behaviour, and peak timing.

Explicit representation of hydraulic structures, especially culverts and bridges, proved crucial for accurately simulating flood routing and timing. In several sub-catchments, the difference between

simplified DEM cut-through methods and structure-aware modelling was not just minor but fundamental. DEM-based simplifications either suppressed discharge peaks or generated unreal flow patterns, whereas explicit culvert modelling captured attenuation effects, delayed responses, and multi-peak hydrographs that better reflect observed system behaviour. This underscores the importance of structure-aware modelling in representing hydraulic constraints and flow diversions in urban settings.

Equally important was the integration of retention basins and pumping stations. The results indicate that flood dynamics in lowland urban catchments cannot be accurately simulated without considering how such infrastructure functions. Simulations based solely on geometric representation consistently underestimated event volumes and distorted recession behaviour. In contrast, employing rule-based discharge–head relationships that reflect real operational practice significantly enhanced the accuracy of peak flows, drawdown phases, and overall hydrograph consistency. However, the remaining peak lag observed under AMC III suggests that accurate operational release alone is insufficient when rapid conveyance through the minor drainage system is implicitly represented. This confirms that operational realism, rather than geometric detail, is a crucial factor in determining the credibility of models in engineered river systems.

The additional R4 calibration step reinforces this conclusion by demonstrating that further improvements in peak timing can be achieved through targeted routing adjustments, but only at the expense of increased volume bias. This confirms that surface roughness calibration can partially compensate for missing fast conveyance pathways, yet cannot fully replace explicit representation of the minor drainage system. Consequently, improvements achieved through routing-focused parameter tuning should be interpreted as indicative of structural model deficiencies rather than as transferable calibration solutions.

The strong interaction between infrastructure performance and antecedent moisture conditions highlights the nonlinear character of urban flood response. Saturated catchment states increase runoff production and significantly modify the effectiveness of pumping and retention systems, while drier conditions cause delayed peaks and lower volumes. These results show that hydrological initialisation is a crucial system state variable and must be explicitly considered when evaluating urban flood hazards and resilience under complex event scenarios.

Taken together, the R4 results indicate that remaining peak timing errors under saturated conditions are not primarily a calibration issue but a structural one, underscoring the need for explicit or reduced-order representations of fast urban conveyance pathways.

Several limitations persist. Sewer surcharge processes were approximated using abstraction terms; subsurface contributions were not explicitly represented, and culvert and bridge blockages were not considered. These simplifications introduce uncertainty and may bias estimates of flood extent, peak attenuation, and local inundation patterns. Addressing these gaps will require closer integration with sewer models (or a simplified dual-drainage approach for inlet exchange, conveyance, and surcharge), systematic inclusion of blockage scenarios, and, where applicable, combined surface–subsurface approaches supported by detailed infrastructure inventories and operational data.

In conclusion, this study shows that reliable urban flood modelling depends on the integrated representation of hydrological states, hydraulic structures, and operational controls within a unified modelling framework. Transfer to neighbouring sub-catchments is most effective when surface parameterisation correlates with observable land-use characteristics and rainfall forcing is similar; it becomes less dependable when calibration is used to account for local drainage connectivity, highlighting the importance of dual-drainage representation for regionalisation. By moving from parameter calibration to structural and operational accuracy, TELEMAT-2D rain-on-grid modelling provides a more credible basis for hazard mapping, risk-informed design, early warning, and scenario-based stress testing of urban water systems. At the same time, the complex nature of urban catchments underscores the importance of scenario-based simulations as a critical area for research and practical application. Such methods enable exploration of compound and cascading conditions,

support uncertainty-aware decision-making, and help bridge the gap between scientific modelling and operational flood risk management, especially when drainage connectivity and control logic are represented with sufficient structural fidelity to facilitate transfer across neighbouring urban catchments.

**Author Contributions:** Conceptualization, JR; methodology, JR, CB, and JH; software, JR; formal analysis, JR; investigation, JR; data curation, JR; writing—original draft preparation, JR; writing—review and editing, JH, AA, and CB; visualization, JR; supervision, CB; project administration, CB; All authors have read and agreed to the published version of the manuscript.

**Funding:** This research was funded by the Interreg North-West Europe Programme through the FlashFloodBreaker project (project ID NWE0200167), co-funded by the European Regional Development Fund (ERDF).

**Data Availability Statement:** Publicly available datasets used in this study are cited in the manuscript. Additional data generated and/or analysed during the current study, including simulation results, are available from the corresponding author upon reasonable request (subject to third-party data restrictions where applicable). Information regarding river gauges, hydraulic infrastructure, and their operational management should be requested from EGLV.

**Acknowledgments:** We gratefully acknowledge Edwin Baumtrog for developing the source code and for his continuous technical support with TELEMAC-2D. We also thank Bernd Böckmann and Valentin Meincke for their ongoing assistance with IT-related issues throughout the project. We sincerely thank Beke Pierick for her substantial contribution through her Master’s thesis, particularly regarding the integration of spatially distributed rainfall. Their collaboration was essential for enabling this work. We also acknowledge that generative AI tools were used to support paraphrasing, data analyses, and the development of evaluation scripts.

**Conflicts of Interest:** The authors declare no conflict of interest.

## Abbreviations

The following abbreviations are used in this manuscript:

AI	Artificial Intelligence
AMC	Antecedent Moisture Conditions
ASCII	American Standard Code for Information Interchange
ATKIS	Authoritative Topographic-Cartographic Information System (Germany; dataset/product name: ATKIS)
CC BY	Creative Commons Attribution License
CFL	Courant–Friedrichs–Lewy condition
CL	Closed configuration (culverts/bridges represented as explicit hydraulic structures)
CN	Curve Number
DEM	Digital Elevation Model
DOI	Digital Object Identifier
DWD	German Weather Service (Deutscher Wetterdienst, DWD)
EGLV	EmscherGenossenschaft and Lippeverband (EGLV; regional water associations)
ERDF	European Regional Development Fund
FEM	Finite Element Method
IT	Information Technology
LiDAR	Light Detection and Ranging
MOC	Method of Characteristics
NSE	Nash–Sutcliffe Efficiency
NRW	North Rhine-Westphalia (NRW, Germany)
OP	Open configuration (structures omitted / “cut-through” representation in the DEM)
QGIS	QGIS (Geographic Information System software)

QP1	Model configuration/scenario label for including retention basins and pumping stations with operational logic (used in “R3+QP1”)
R <sup>2</sup>	Coefficient of determination
R1–R4	Calibration / model-development stages (R1 baseline → later stages with increasing structural/infrastructure representation and routing focus)
RADOLAN-RW	RADOLAN radar precipitation product (RW variant)
RMSE	Root Mean Square Error
RWTH	RWTH Aachen University
SCS	Soil Conservation Service
SCS-CN	Soil Conservation Service Curve Number method
SUPG	Streamline Upwind Petrov–Galerkin

## Appendix A

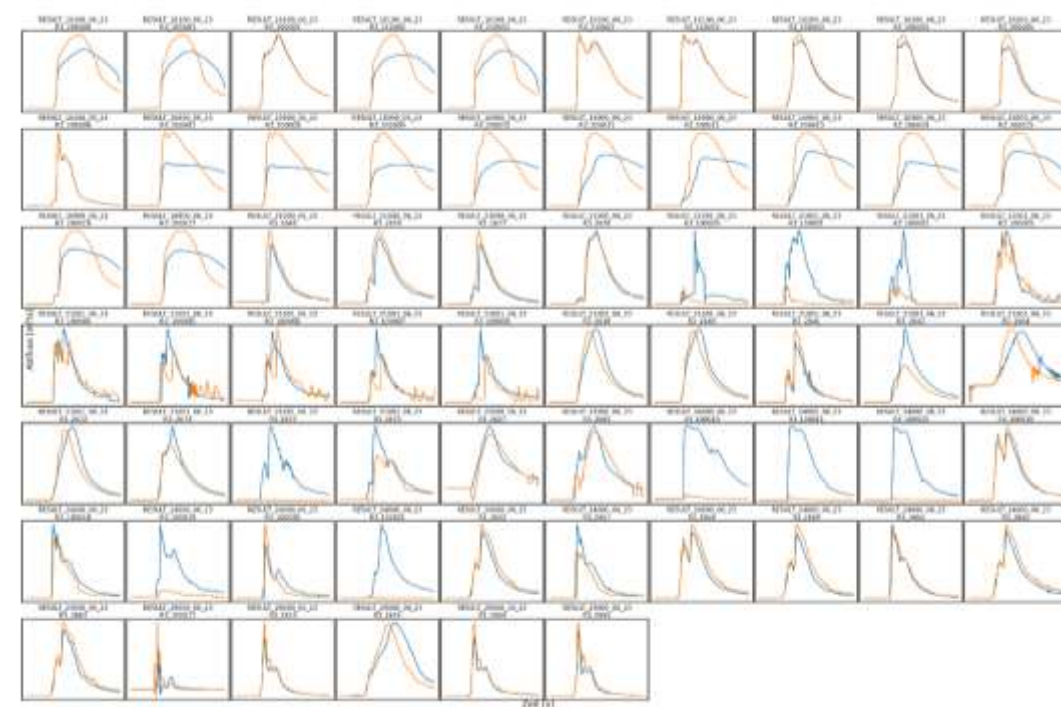


**Figure A1.** Discharge hydrograph comparison (open vs. closed) at 66 culvert and bridge locations across the subcatchments of Rossbach and Rüpingsbach in the Emscher catchment area.

## References

1. Milly, P.C.D.; Wetherald, R.T.; Dunne, K.A.; Delworth, T.L. Increasing risk of great floods in a changing climate. *Nature* 2002, 415, 514–517, doi:10.1038/415514a.
2. Smolders, S.; Leroy, A.; Teles, M.J.; Maximova, T.; Vanlede, J. Culverts modelling in TELEMAC-2D and TELEMAC-3D. In *Proceedings of the XXIIIrd TELEMAC-MASCARET User Conference 2016, 11 to 13 October 2016, Paris, France*; Bourban, S., Ed.; HR Wallingford: Oxfordshire, 2016; p 21.
3. Broich, K.; Pflugbeil, T.; Disse, M.; Nguyen, H. Using TELEMAC-2D for Hydrodynamic Modeling of Rainfall-Runoff. In *XXVIth TELEMAC-MASCARET User Conference, 15th to 17th October 2019, Toulouse*; CNRS/CERFACS, 2019.
4. Vos, L.F. de; Rütther, N.; Mahajan, K.; Dallmeier, A.; Broich, K. Establishing Improved Modeling Practices of Segment-Tailored Boundary Conditions for Pluvial Urban Floods. *Water* 2024, 16, 2448, doi:10.3390/w16172448.

5. Salvisberg, R.; Marti, T.; Arrigo-Meier, S.; Petar, M. Flood risk management based on 2D TELEMAC computations: an example with Swiss hazard map. In *XXVIIth TELEMAC-MASCARET User Conference, 15th to 17th October 2019, Toulouse*; CNRS/CERFACS, 2019.
6. Ligier, P.-L. Implementation of a rainfall-runoff model in TELEMAC-2D. In *Proceedings of the XXIIIrd TELEMAC-MASCARET User Conference 2016, 11 to 13 October 2016, Paris, France*; Bourban, S., Ed.; HR Wallingford: Oxfordshire, 2016; p 13.
7. Adouin, Y.; Moulinec, C.; Barber, R.; Sunderland, A. Preparing TELEMAC-2D for extremely large simulations. In *Proceedings of the XVIIIth Telemac & Mascaret User Club 2011, 19-21 October 2011, EDF R&D, Chatou*; Violeau, D., Hervouet, J.-M., Razafindrakoto, E., Denis, C., Eds.; EDF R&D: Chatou, 2011; p 35.
8. Guo, K.; Guan, M.; Yu, D. Urban surface water flood modelling – a comprehensive review of current models and future challenges. *Hydrol. Earth Syst. Sci.* **2021**, *25*, 2843–2860, doi:10.5194/hess-25-2843-2021.
9. Leandro, J.; Schumann, A.; Pfister, A. A step towards considering the spatial heterogeneity of urban key features in urban hydrology flood modelling. *Journal of Hydrology* **2016**, *535*, 356–365, doi:10.1016/j.jhydrol.2016.01.060.
10. Xing, Y.; Chen, H.; Liang, Q.; Ma, X. Improving the performance of city-scale hydrodynamic flood modelling through a GIS-based DEM correction method. *Nat Hazards* **2022**, *112*, 2313–2335, doi:10.1007/s11069-022-05267-1.
11. Zhang, J.; Wu, G.; Liang, B.; Chen, Y. Subgrid modeling of urban flooding incorporating buildings' effects. *Physics of Fluids* **2023**, *35*, doi:10.1063/5.0178816.
12. Wang, Y.; Chen, A.S.; Fu, G.; Djordjević, S.; Zhang, C.; Savić, D.A. An integrated framework for high-resolution urban flood modelling considering multiple information sources and urban features. *Environmental Modelling & Software* **2018**, *107*, 85–95, doi:10.1016/j.envsoft.2018.06.010.
13. Ah-Woane, E.; Amama, Z.; Cordier, F.; Davarend, T.; Lotfi, J.; Assaba, M.; Sochinskii, A.; Majdalani, S.; Moussa, R.; Abily, M.; et al. Toward Brague river flood modelling 3: the impact of culvert representation. *Digital Water* **2025**, *3*, 1–22, doi:10.1080/28375807.2025.2465376.
14. Lee, J.-H.; Lee, S.; Kim, B.; Choi, H.; Noh, S.J. Evaluating the Effects of Spatial Resolution on 2D Pluvial Flood Modeling in Urban Built Environments. *J Flood Risk Management* **2025**, *18*, doi:10.1111/jfr3.70105.
15. Butters, O.; Robson, C.; McClean, F.; Glenis, V.; Virgo, J.; Ford, A.; Iliadis, C.; Dawson, R. An open framework for analysing future flood risk in urban areas. *Environmental Modelling & Software* **2025**, *185*, 106302, doi:10.1016/j.envsoft.2024.106302.
16. Mignot, E.; Li, X.; Dewals, B. Experimental modelling of urban flooding: A review. *Journal of Hydrology* **2019**, *568*, 334–342, doi:10.1016/J.JHYDROL.2018.11.001.
17. Hettiarachchi, S.; Wasko, C.; Sharma, A. Can antecedent moisture conditions modulate the increase in flood risk due to climate change in urban catchments? *Journal of Hydrology* **2019**, *571*, 11–20, doi:10.1016/j.jhydrol.2019.01.039.
18. Godara, N.; Bruland, O.; Alfredsen, K. Modelling Flash Floods Driven by Rain-on-Snow Events Using Rain-on-Grid Technique in the Hydrodynamic Model TELEMAC-2D. *Water* **2023**, *15*, 3945, doi:10.3390/w15223945.
19. Godara, N.; Bruland, O.; Alfredsen, K. Simulation of flash flood peaks in a small and steep catchment using rain-on-grid technique. *J Flood Risk Management* **2023**, *16*, doi:10.1111/jfr3.12898.
20. Bourban, S.E.; Turnbull, M.S. A simplified approach to modelling all types of obstacles in TELEMAC-2D and 3D. In *Proceedings of the XXIXth TELEMAC Users Conference 12-13 October 2023*; Kopmann, R., Folke, F., Eds.; Bundesanstalt für Wasserbau: Karlsruhe, 2023; p 217.
21. Mignot, E.; Dewals, B. Hydraulic modelling of inland urban flooding: Recent advances. *Journal of Hydrology* **2022**, *609*, 127763, doi:10.1016/j.jhydrol.2022.127763.

**Disclaimer/Publisher's Note:** The statements, opinions and data contained in all publications are solely those of the individual author(s) and contributor(s) and not of MDPI and/or the editor(s). MDPI and/or the editor(s) disclaim responsibility for any injury to people or property resulting from any ideas, methods, instructions or products referred to in the content.